Research Report

A Phenomenological Multi-zone PDF Model to Predict Transient Behavior of Diesel Engine Combustion

Kazuhisa Inagaki, Matsuei Ueda, Jun'ichi Mizuta, Kiyomi Nakakita and Shigeki Nakayama

Report received on Sep. 27, 2011

ABSTRACT A novel engine cycle-simulation program has been developed to reproduce the diesel combustion process for wide changes in engine operating parameters, such as injected fuel quantity, injection timing, and EGR ratio. The approach described in this paper employs a zoning model, where the in-cylinder region is divided into a maximum of 5 zones. A Probability Density Function (PDF) concept is also applied to each zone to consider the effect of spatial inhomogeneities, such as local equivalence ratios and temperature, on the combustion characteristics. This program was linked to the generally used commercial GT-Power® software. As a result, transient engine behavior was reproduced very accurately.

KEYWORDS Compression Ignition Engine, Diesel Engine, Modeling, Simulation, Combustion Control

1. Introduction

Diesel engine vehicles have been gaining greater market penetration as environmental issues gain prominence around the world, especially in Europe and Asia, because of their good fuel economy. Unfortunately, diesel engines emit more soot and nitrogen oxides (NOx) than gasoline engines, and reducing these emissions while maintaining a high thermal efficiency presents an urgent and major challenge. In recent years, Low Temperature Combustion (LTC),[1] Modulated Kinetics (MK),[2] and Homogeneous Charge Compression Ignition (HCCI)[3] have become the focus of engine research around the world due to advantages such as high thermal efficiency and very low NOx and soot emissions. These types of engines have great potential to gain acceptance as a way of meeting challenging future emission regulations. However, the combustion robustness of these engines is relatively poor owing to the use of a larger amount of EGR gas than in conventional diesel combustion. In addition, the switching between clean high-EGR and conventional combustion modes that will be required during transient operation is very difficult to control, because engine control parameters such as EGR ratio and injection timing change in a discontinuous manner throughout the mode-switching process. To solve the above problems, it is necessary to develop a novel combustion controlling system. Forming an understanding of the transient cycle-to-cycle combustion process is the key to effective and fast development of such a system.

Under this background, the purpose of this study was to construct a unique method of engine cycle-simulation to enable accurate prediction of engine transient performance within a reasonable calculation time. It was clarified that the developed simulation can be applied to the prediction of combustion performance in a wide range of engine operating conditions, using a newly developed multi-zone model that employs the Probability Density Function (PDF) concept.

2. Simulation Method

Recently, 3D-CFD has become the general method of reproducing the in-cylinder combustion process. However, because it often needs much time to execute, typically some hours to a few days for a single engine-cycle calculation, it is not a practical method of predicting transient behavior over several tens of engine cycles. On other hand, 0D engine cycle-simulations have been introduced together with some phenomenological spray and combustion models.[4,5] While execution time is much shorter than with 3D-CFD, a key issue is how accurately prediction can be made with such a spatially simplified 0D-model. To meet both accuracy and time requirements, a multi-

Reprinted from Review of Automotive Engineering, Vol.28, No.3, pp.337-344, © 2007 JSAE, with permission from Society of Automotive Engineers of Japan.

zone model combined with a PDF concept has been developed, which was designed to cover cases of multi-injection using double pilots and single main injections. The principal models are summarized in **Table 1**. Each model is detailed in the following section.

2. 1 Zoning Model

Figure 1 illustrates an outline of the zoning model. In the model, in-cylinder volume is divided into an air zone (Zone 2), and a spray zone. The spray zone is sub-divided into two regions, Zone 1 and Zone 3. Zone 1 is formed during fuel injection before ignition, and Zone 3 after ignition. These correspond to the so-called premixed and diffusive combustion zones, respectively. According to the model, if ignition occurs after injection, only Zone 1 is formed as the spray zone. Ignition timing is defined as the timing when the temperature of Zone 1 exceeds 1000 K. Until ignition begins, the air is transferred from Zone 2 (air zone) to Zone 1, while fuel droplets are injected into Zone 1. Then, once ignition occurs, both air and fuel droplets are introduced into Zone 3 in turn. The entrained air volume is calculated based on the Hiroyasu equations[6] shown in Eq. (1) to (4), together with an assumption that the spray shape is a simple circular cone with a height of spray penetrating length expressed in Eq. (1), and with a cone angle in Eq. (2).

$$S = \begin{cases} 0.39\sqrt{2\Delta P/\rho_f}\cdot t & (0 \le t \le t_b) \\ 2.95\left(\Delta P/\rho_a\right)^{0.25}\sqrt{d_0 t} & (t > t_b) \end{cases} \quad [\mathrm{m}] \cdots (1)$$

$$\theta = 0.05\left(\frac{\rho_a \Delta P d_0^{\,2}}{\mu_a^{\,2}}\right) \quad [\mathrm{deg.}] \cdots (2)$$

$$V_{spray} = \frac{1}{3}\pi \tan^2\theta \cdot S^3 \quad [\mathrm{m}^3] \cdots (3)$$

$$dV_{air} = \frac{dV_{spray}}{dt}\cdot \Delta t \quad [\mathrm{m}^3] \cdots (4)$$

where, S: spray penetrating length, ΔP: pressure difference between injection and ambient pressures, ρ_f: fuel density, t_b: droplet breakup time, ρ_a: ambient density, d_0: injection nozzle orifice diameter, θ: spray full cone angle, μ_a: air viscosity, V_{spray}: spray volume, Δt: time step.

Fuel droplets are treated according to the Discrete Droplet Model (DDM), droplet size is obtained from Kawamura's equation,[7] and fuel vaporization is modeled by Spalding's model.[8]

2. 2 Probability Density Function (PDF) Model

A zoning model is not sufficient enough by itself to reproduce a real diesel combustion process accurately, because the inside of a spray contains a wide range of fuel concentration distribution, and its inhomogeneity that changes temporally and spatially must be modeled. A PDF model is appropriate to express such a changing heterogeneous condition.[9] However, since a large increase in execution time would be a drawback, a new and very simple PDF model aiming

Table 1 Models used in cycle-simulation.

Fuel injection process	Multi-zone model
Local inhomogeneity of mixture	PDF model
Air entrainment	Hiroyasu model[6]
Droplet size	Kawamurâs equation[7]
Droplet evapolation	Spalding model[8]
Ignition	Multi-step shell model[10]
Combustion	Kong model[11]
Turbulence	Ikegami model[9]
Bulk flow (Swirl/Squish flow)	Arai model[12]
Heat-loss	Woschni model[13]
Combustion noise calculation	Taki model[14]

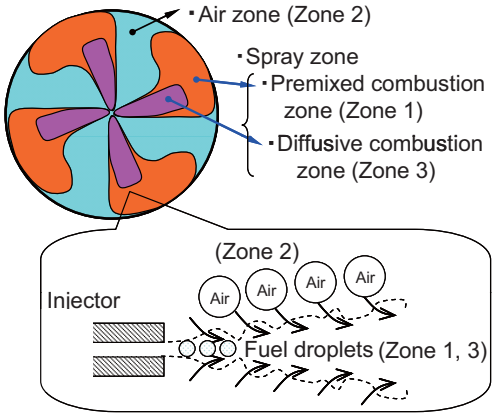

Fig. 1 Schematics of zoning model
(Zone 1: premixed combustion zone of spray,
Zone 2: air zone,
Zone 3: diffusive combustion zone of spray).

at fast calculation is proposed as described below, and is linked to the zoning model.

Figure 2 shows an outline of the PDF model. In the PDF model, the mixture within each zone is treated as a cluster of discrete mixture fragments, which are called packages. In the first stage, entrained air designated by the terms G_i (fuel vapor mass fraction $f_v = 0$) and fuel vapor G_j ($f_v = 1$), exist independently in a spray zone, as shown on the left side of Fig. 2. During time step Δt, G_i and G_j are mixed partially and G_k that has a different fuel mass fraction ($0 < f_v < 1$) is newly formed, as shown on the right side. Such mixing between packages results in a probability density function in terms of the fuel vapor mass fraction or equivalence ratio. G_i as air and G_j as fuel vapor are continuously introduced into the spray zone during the injection period.

It should be emphasized that the key point of the PDF model is how to define the mixing rate between packages. In this model, mixing mass $\Delta M_{i,j}$ between G_i and G_j during Δt is given by Eq. (5) and (6).

$$\Delta V_{sweep} = 0.25\pi \cdot d^2{}_j \left| v_j - v_i \right| \cdot \Delta t \qquad [\mathrm{m}^3] \cdots (5)$$

$$\Delta M_{i,j} = \alpha \cdot \rho \cdot \Delta V_{sweep} \cdot V_i / \sum V_l \qquad [\mathrm{kg}] \cdots (6)$$

where, d_j: equivalent spherical diameter that has the same volume as G_j, v_j: velocity of G_j, ΔV_{sweep}: volume swept by G_j over G_i during Δt, V_i: volume of G_i, ρ: mixture density, α: adjustment parameter of mixing rate.

The subscript i is given to the larger gas package in terms of volume, and j to the smaller. The volume swept by G_j during Δt, or ΔV_{sweep}, is calculated as a cylindrical volume from Eq. (5). $\Delta M_{i,j}$ is simply assumed to be proportional to ΔV_{sweep}, the ratio of V_i to the whole spray volume and Δt. New masses of G_i, G_j and G_k are obtained respectively by Eq. (7) so that the total mass is conserved. Similarly, new velocity v_k, fuel mass fraction f_k and enthalpy h_k of gas package G_k after mixing are given by Eq. (8), (9) and (10) so that the total momentum, fuel mass and enthalpy are conserved, respectively.

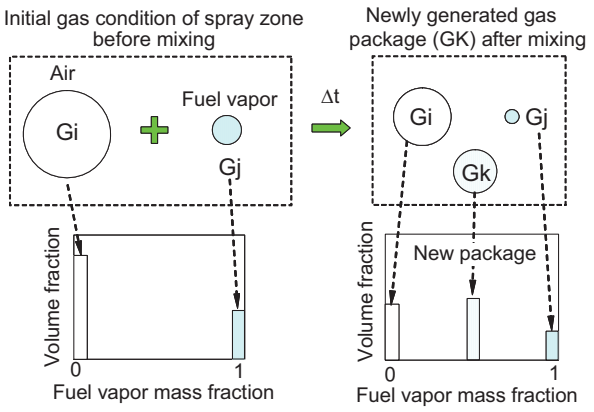

Fig. 2 Image of air/fuel mixing process using PDF gas package model.

$$M_i^{n+1} = M_i^n - \Delta M_{i,j} \qquad M_j^{n+1} = M_j^n - \Delta M_{i,j} \qquad M_k^{n+1} = M_k^n + 2\Delta M_{i,j}$$
$$[\mathrm{kg}] \cdots (7)$$

$$f_k^{n+1} = \left(f_k^n \cdot M_k + f_i^n \cdot \Delta M_{i,j} + f_j^n \cdot \Delta M_{i,j}\right) \Big/ \left(M_k^n + 2\Delta M_{i,j}\right) \cdots (8)$$

$$v_k^{n+1} = \left(v_k^n \cdot M_k + v_i^n \cdot \Delta M_{i,j} + v_j^n \cdot \Delta M_{i,j}\right) \Big/ \left(M_k^n + 2\Delta M_{i,j}\right)$$
$$[\mathrm{m/s}] \cdots (9)$$

$$h_k^{n+1} = \left(h_k^n \cdot M_k + h_i^n \cdot \Delta M_{i,j} + h_j^n \cdot \Delta M_{i,j}\right) \Big/ \left(M_k^n + 2\Delta M_{i,j}\right)$$
$$[\mathrm{J/kg}] \cdots (10)$$

As initial values, injection velocity is set to v_j of the pure fuel package G_j, and zero is set to v_i of the pure air package G_i. α in Eq. (6) is an adjustment constant parameter related to mixing efficiency. Once α was tuned for a certain engine operating condition so as to match the corresponding measured heat release rate, it was kept constant even for the other different conditions in order to assess the robustness of predictability.

2. 3 Ignition and Combustion Model

Shell model[10] is used until the temperature of gas package exceeds 1000 K, and a simplified version of the Laminar-Turbulence Characteristic Time Combustion (LTCTC)[11] model is used after 1000 K, as shown in Eq. (11)

$$\frac{dY_f}{dt} = -\frac{Y_f}{\tau_c}$$
$$\begin{cases} \tau_l = 1/\left([fuel][O_2]\exp\left(-E/RT\right)\right) \\ \tau_t = C_2 \cdot k/\varepsilon \\ \tau_c = \tau_l + f \cdot \tau_t \end{cases} \cdots (11)$$

where, Y_f: fuel mass fraction, τ_l: laminar characteristic time, τ_t: turbulent characteristic time, k: turbulent kinetic energy, ε: dissipation of turbulence kinetic energy.

Turbulent kinetic energy k and its dissipation ε is calculated by the Ikegami model,[9] as shown in Eq. (12)

$$\frac{dk}{dt} = G_j + G_s - \varepsilon - k \cdot \frac{d(\ln(M))}{dt}$$
$$\varepsilon = \left(2k/3\right)^{1.5} \Big/ L_j, \qquad G_j = \left(\eta_j / 2M\right) \cdot \dot{m}_f u_j^{\,2},$$
$$G_s = \left(\eta_s u_s\right)^3 / L_j, \qquad L_j = \left(\rho_f / \rho_a\right)^{0.5} d_0$$
$$\cdots\cdots\cdots\cdots (12)$$

where, M: total mass of spray zone, $\dot{m}_f$: injection mass rate, u_j: injection velocity

2. 4 Extended Multi-Zone Model for Multi-injections

In the latest diesel engines, a multi-injection strategy is used with a common rail injection system to improve emissions performance. In order to analyze such multi-injection strategies up to double-pilot and single main injections, an extended version of the multi-zone model was developed, as shown in **Fig. 3**. Zone 4 and 5 are newly introduced to express the 1st pilot and 2nd pilot sprays, respectively. In the multi-injection case, gas is entrained into the spray zone from not only the air zone (Zone 2), but also the other spray zones. As an example, the main spray (Zone 1) has 1st pilot (Zone 4) and 2nd pilot (Zone 5) sprays as source zones for gas entrainment besides the air zone (Zone 2), as shown in Fig. 3. The quantity of burned gas from the pilot zones included in the total volume of the gas entrained into the main spray is important, because this can affect the main spray temperature and then the following ignition event. In this study, each percentage of the gas originating in the pilot and air zones in the total entrained gas is given proportionally to each volume fraction for the pilot zone and air zone.

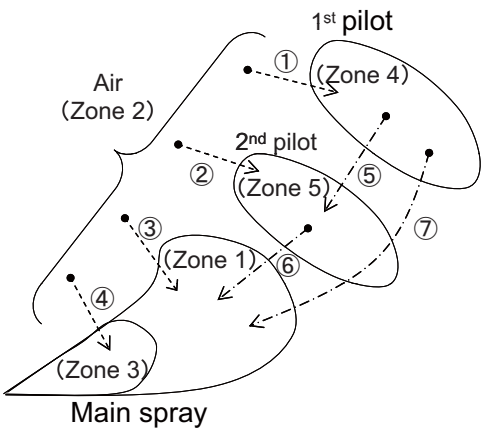

Fig. 3 Schematics of zoning model for multiple injection
(Zone 1: premixed combustion zone of main spray,
Zone 2: air zone,
Zone 3: diffusive combustion zone of main spray,
Zone 4: 1st pilot spray zone,
Zone 5: 2nd pilot spray zone).

2. 5 Other Physical Models

In-cylinder gas motions of swirl and squish flows are modeled by Arai's Method[12] to account for the effects of gas flows on the gas entrainment of the spray. Heat loss from the in-cylinder gas to the wall is accounted by the Woschni model,[13] considering the swirl flow effect. Combustion noise is calculated by the Taki model[14] from simulated pressure traces. Consequently, the simulation has the same functions as the AVL Combustion Noise Meter commonly used in engine experiments, and diesel or HCCI knocking is also predictable.

2. 6 Linked to GT-Power® for More Realistic Engine Simulation

This cycle-simulation with a multi-zone PDF model was linked to the commercial software code GT-Power® in order to conduct more realistic engine simulations. As a result, it became possible to model intake and exhaust strokes with actual pipes and engine accessory components such as turbo-chargers and the EGR system. **Figure 4** shows an example of an engine model. In this linked version, the cycle-simulation is used during the compression and expansion strokes, which is the period from the closing of the intake valves to just before the opening of the exhaust valves. When the switch occurs between the cycle-simulation and GT-Power®, gas properties such as mass, velocity and enthalpy are inherited. The efficiency map for a turbo-charger was obtained from Uchida's program.[15] This version was used to demonstrate an analysis for transient behavior from a conventional combustion mode to HCCI mode, as described later.

3. Results

3. 1 Predictability of Diesel Combustion Process by Multi-zone PDF Model

Experiments were conducted using a single cylinder diesel engine to examine the predictability of the diesel combustion process by the proposed multi-zone PDF model. The engine specifications are listed in **Table 2**. Some combustion control parameters such as injection quantity, injection timing and injection pressure were changed widely, and in-cylinder pressure based analyses were performed. HCCI experiments using intake port injection of n-pentane fuel were also conducted with the same engine.

Figure 5 shows the effect of the PDF model parameter α in Eq. (6) on the simulated heat release rate. The quantity of injection fuel was 36 mm^3/st. In the case of a larger α, fuel-air mixing is enhanced and the mixture becomes more diluted, as shown in the PDF graph in Fig. 5. It causes a shorter ignition delay and a decrease in the 1st peak of heat release rate in the premixed combustion, as shown in the figure. When $\alpha = 0.414$, the simulated heat release rate agrees well with the measurement. Therefore this α value is used even for the other engine conditions to assess the robustness of the PDF model.

Figure 6 shows the temperature change of each gas package in relation to the equivalence ratio φ and crank angle under the same conditions as Fig. 5. At around 1 degree ATDC before ignition, the fuel-rich gas package decreases in temperature (Fig. 6 area A) owing to the latent heat of fuel evaporation. Ignition starts from near

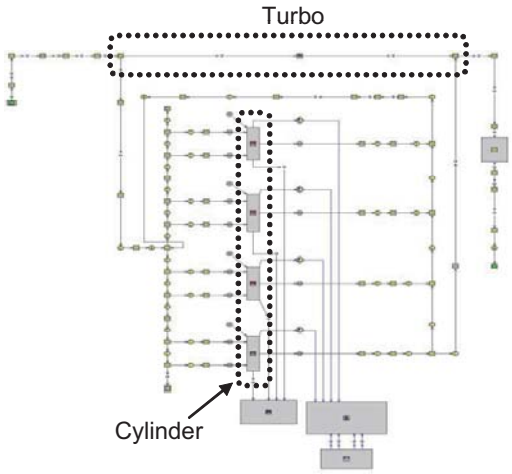

Fig. 4 Engine model of GT-POWER®.

Table 2 Engine specifications.

Engine type	Single cylinder, 4 cycle
Bore × Stroke	96 mm × 103 mm
Displacement	750 cc
Compression ratio	16
Combustion chamber shape	Shallow-dish type
Fueling system (direct inj.)	Common rail type
Injector hole size × num.	φ0.15 mm × 7
Swirl ratio	2.3

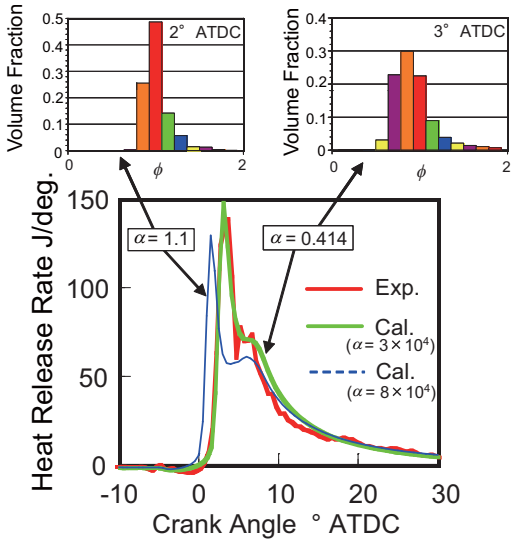

Fig. 5 The effect of mixing efficiency α in PDF model. Upper figures show histograms of volume fraction regarding equivalence ratio φ, lower figure shows heat release rate with changes in α (amount of injected fuel: 37 mm^3/st., injection timing: –4.5° ATDC, engine speed: 1200 rpm).

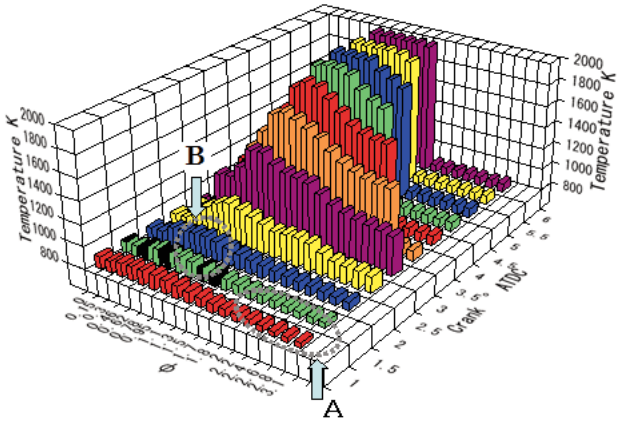

Fig. 6 Changes in temperature vs. φ of gas mixtures of PDF model.

stoichiometric conditions (Fig. 6 area B) at around 2 degrees ATDC, and then the other packages rapidly increase in temperature due to mixing of the gas packages. For this single injection case, execution time is about 30 sec./cycle on a PC, which is fast enough to analyze engine transient behavior over several hundred cycles.

Figure 7 shows the effect of the quantity of injection fuel on the heat release rate. In the experiment (upper figure), the ignition timing is slightly advanced as fuel quantity increases. When this occurs, the first peak of the heat release rate is smaller and the second peak of diffusive combustion appears clearer. This shorter ignition delay is caused by the effect that burned gas residue in the cylinder, i.e., internal EGR gas, increases the intake gas temperature of the following cycle as the fuel quantity is increased. To account for this in the simulation, internal EGR gas with a certain volume fraction is mixed with the intake air through a multi-cycle calculation. Consequently, the simulated results show good agreement with measurement, as shown in Fig. 7. Therefore, it was found that the models can predict the combustion process accurately when the injection fuel amount changes.

Figure 8 shows the effect of injection pressure on the heat release rate. In the experiment (upper figure), the heat release rate peak became much higher as the injection pressure increased. It was found that the simulation reproduces this very well. **Figure 9** shows simulated histograms of volume fraction for an equivalence ratio φ at 4 degrees ATDC. In the case of higher injection pressure, φ distributions are shifted to the leaner side, and the enhancement of air entrainment with increased injection pressure can be reproduced well.

Figure 10 shows the effect of injection timing on the heat release rate. In the experiment (upper figure), the ignition delay became shorter as the injection timing was retarded because the ambient temperature is higher at injection. It results in a smaller heat release rate peak. On the other hand, when the injection timing is retarded further, ignition delay becomes longer because the ambient temperature is lower at injection, resulting in a larger peak. These trends are predicted accurately by the simulation.

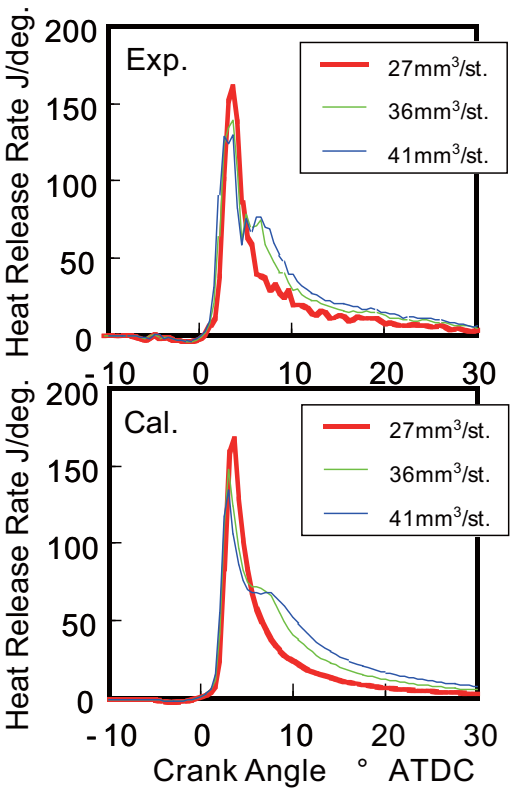

Fig. 7 Effect of quantity of injection fuel on heat release rate (upper: experiment, lower: calculation).

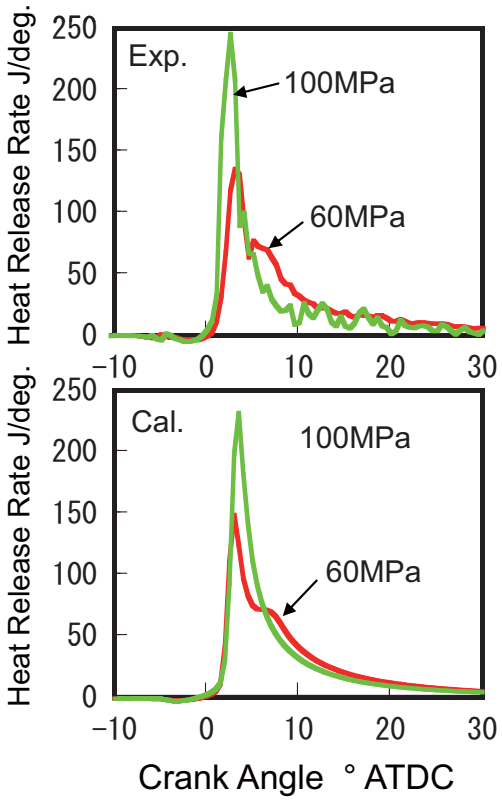

Fig. 8 Effect of injection pressure on heat release rate (upper: experiment, lower: calculation).

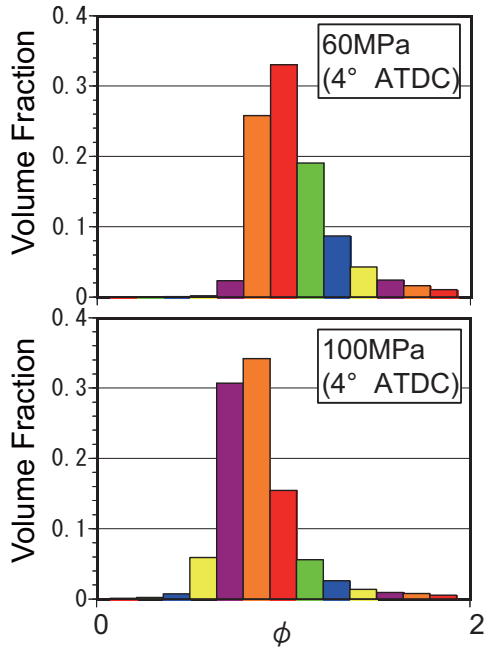

Fig. 9 Comparison of histograms of equivalence ratio φ between 60 MPa and 100 MPa of injection pressure calculated by PDF model.

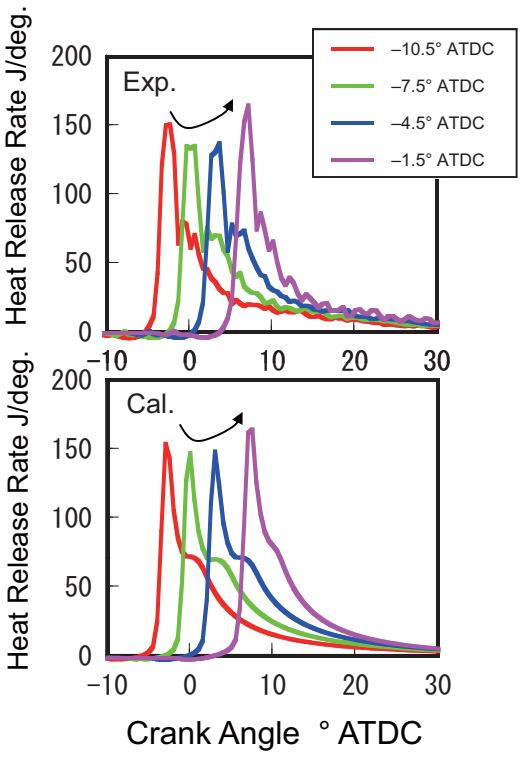

Fig. 10 Effect of injection timing on heat release rate (upper: experiment, lower: calculation).

3. 2 Predictability of Extended Multi-zone Model for Multi-injections

Figure 11 shows an example of a case of multi-injection using the 5-zone model explained in Section 2.4. The figure also shows the injection periods for the 1st & 2nd pilots and main injections. It demonstrates an excellent agreement between the experimental and simulated heat release rates. Although it takes more time, i.e., a few minutes, for a case of multi-injection than a case of single injection, it can still be applied to conduct a multi-cycle simulation. Major issues for future work include whether the model is applicable to a wide change of injection parameters, such as intervals between pilot-to-pilot and pilot-to-main injections, and pilot fuel amounts.

3. 3 Predictability of HCCI Combustion Characteristics

This section assesses the predictability of HCCI combustion characteristics. **Figure 12** shows the effect of the EGR ratio on the heat release rates of HCCI. In the experiment (upper figure), as the EGR ratio increased, the heat release rate in Low Temperature Oxidation (LTO) fell and the ignition timing was retarded while the High Temperature Oxidation (HTO) peak became lower. It was found that these trends could be predicted well.

Figure 13 shows a comparison of HCCI combustion noise between experiment and simulation. There is a good agreement between experiment and simulation in terms of the trend where combustion noise is reduced

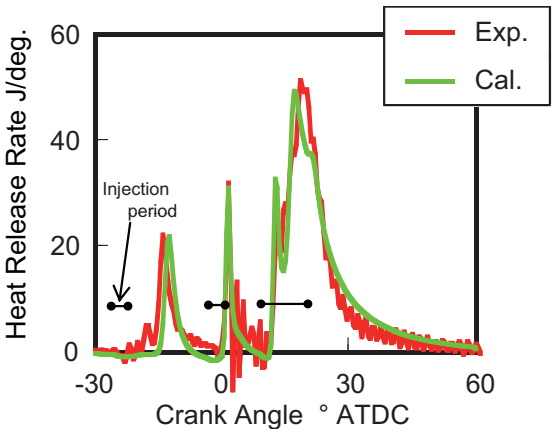

Fig. 11 Comparison of heat release rate between experiment and calculation for case of multiple fuel injection.

as the EGR rate increases. This means that HCCI knocking, which is one of the biggest problems for real world application, is predictable. Good agreement was also found for changes in intake gas pressure, temperature, and injection fuel amount, although lack of space prevents the display of the applicable graphs.

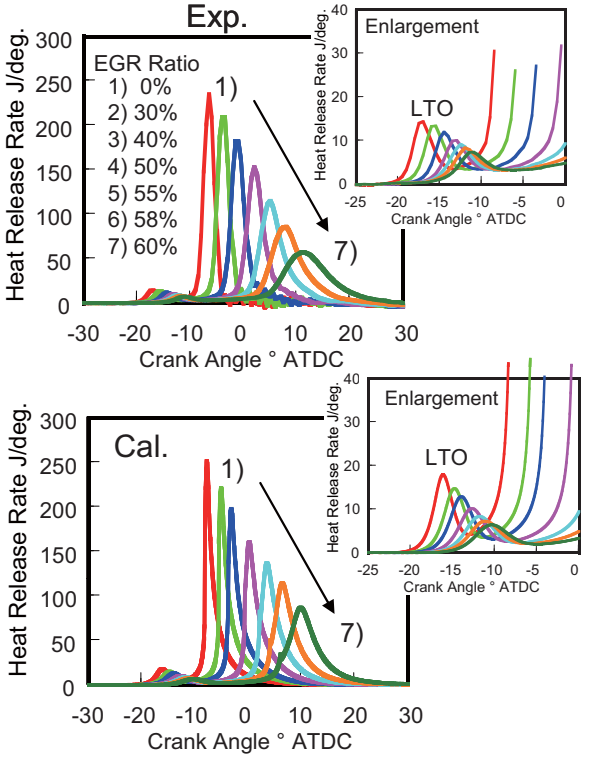

Fig. 12 Effect of EGR ratio on heat release rate of HCCI (upper: experiment, lower: calculation).

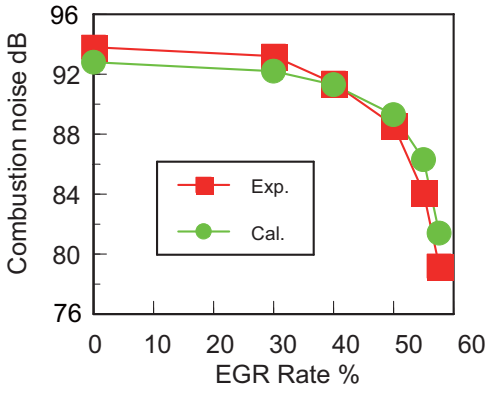

Fig. 13 Comparison of combustion noise between experiment and calculation with changes in injection pressure.

3. 4 Analysis for Transient Behavior from Conventional Mode to HCCI Mode

Figures 14 and **15** show transient behavior during a switch from a conventional combustion mode to HCCI mode simulated by the version of the simulation linked to GT-Power®. As soon as the switch to HCCI mode occurs, injection timing advances widely from –4.5 to –40 degrees ATDC, and the EGR valve is opened to achieve a target EGR ratio of 70%. Because the EGR ratio cannot reach this target immediately, the heat release rate of HCCI sharply increases just after the switch occurs, and then combustion relaxes gradually, as shown in the figures. This is typical of HCCI knocking, which is one of the largest problems facing practical use of this type of engine.

As demonstrated above, the simulation can predict transient engine performance well. In the next stage, it is planned to develop a novel control system together with the simulation tool to solve problems related to HCCI.

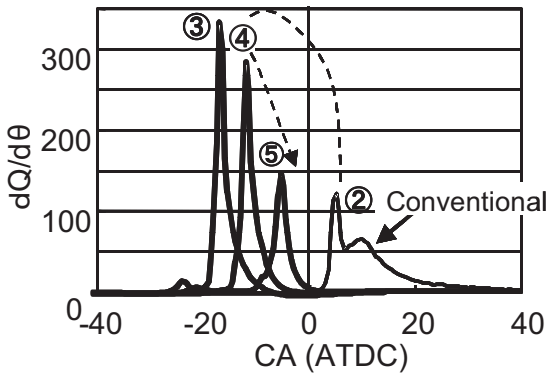

Fig. 14 Transient change of heat release rate during switch from conventional combustion mode to HCCI mode.

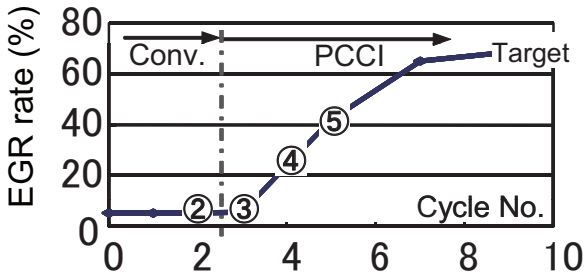

Fig. 15 Transient change of EGR ratio during switch from conventional combustion mode to HCCI mode.

4. Summary

A novel engine cycle-simulation program has been developed to reproduce both conventional diesel and HCCI combustion for wide changes in engine operating conditions. The principal results are as follows:

(1) Combustion characteristics were predicted well for wide changes in fuel injection quantity, injection pressure, and injection timing by the simulation that uses a multi-zone PDF model.
(2) The combustion process of multi-injection (double pilots and single main injections) is also accurately predictable with the extended 5-zone model.
(3) The model is also applicable to HCCI combustion.
(4) Execution time is a few minutes/cycle for cases of multi-injection case on a PC, which is acceptable for simulating multi-cycle transient engine performance.
(5) A version that is linked to GT-Power® software allows more realistic engine simulations, and accurate prediction of HCCI knocking when the switch occurs from a conventional combustion mode to HCCI mode.

References

(1) Akihama, K., Takatori, Y., Inagaki, K., Sasaki, S. and Dean, A. M., "Mechanism of the Smokeless Rich Diesel Combustion by Reducing Temperature", *SAE Tech. Paper Ser.*, No.2001-01-0655 (2001).
(2) Kimura, S., et al., "Ultra-clean Combustion Technology Combining Low-temperature and Premixed Concept to Meet Future Emission Standards", *SAE Tech. Paper Ser.*, No.2001-01-0200 (2001).
(3) Hasegawa, R. and Yanagihara, H., "HCCI Combustion in DI Diesel Engine", *SAE Tech. Paper Ser.*, No.2003-01-0745 (2003).
(4) Hiroyasu, H. and Kadota, T., "Models for Combustion and Formation of Nitric Oxide and Soot in Direct Injection Diesel Engines", *SAE Tech. Paper Ser.*, No.760129 (1976).
(5) Barbara, C., et al., "Phenomenological Combustion Model for Heat Release Rate Prediction in High-speed DI Diesel Engine with Common Rail Injection", *SAE Tech. Paper Ser.*, No.2001-0102933 (2001).
(6) Hiroyasu, H. and Arai, M, "Fuel Spray Penetration and Spray Angle in Diesel Engine (in Japanese with English Summary)", *JSAE*, No.21 (1980), pp.5-11.
(7) Kawamura, K. and Saito, A., *The 2nd Atomization Symposium* (1993), pp.115-120.
(8) Spalding, D. B., *Proc. 4th Symposium (International) on Combustion* (1952), p.847.
(9) Ikegami, M., Shioji, M. and Koike, M., "A Stochastic Approach to Model the Combustion Process in Direct-injection Diesel Engines", *Twentieth Symposium (International) on Combustion* (1984), pp.217-224, the Combustion Institute.
(10) Halstead, M. P., Kirsch, L. J. and Quinn, C. P., "The Autoignition of Hydrocarbon Fuels at High Temperatures and Pressures-fitting of a Mathematical Model", *Combustion and Flame*, Vol.30 (1977), pp.45-60.
(11) Kong, S.-C., Han, Z. and Reitz, R. D., "The Development and Application of a Diesel Ignition and Combustion Model for Multidimensional Engine Simulation", *SAE Tech. Paper Ser.*, No.950278 (1995).
(12) Murakami, A., Arai, M. and Hiroyasu, H., "Swirl Measurements and Modeling in Direct Injection Diesel Engines", *SAE Tech. Paper Ser.*, No.880385 (1988).
(13) Sihling, K. and Woschni, G., "Experimental Investigation of the Instantaneous Heat Transfer in the Cylinder of a High Speed Diesel Engine", *SAE Tech. Paper Ser.*, No.790833 (1979).
(14) Taki, M., Takasu, S. and Akihama, K., "Effect of Combustion Period on HCCI Combustion Noise (in Japanese with English Summary)", *Procceedings of JSAE*, No.20065179 (2005).
(15) Uchida, H., et al., "Transient Performance Prediction of the Turbocharging System with Variable Geometry Turbochargers", *8th International Conference on Turbochargers and Turbocharging*, C647/018 (2006), I MechE.

Kazuhisa Inagaki
Research Field:
- Diesel Engine Combustion

Academic Societies:
- The Japan Society of Mechanical Engineers
- Society of Automotive Engineers of Japan

Awards:
- Outstanding Technical Paper Award of JSAE, 2004, 2005, 2009 and 2010
- SAE 2003 Harry LeVan Horning Memorial Award, 2004

Matsuei Ueda
Research Fields:
- Exhaust Aftertreatment
- Diesel Engine Combustion

Academic Degree: Dr. Eng.
Academic Societies:
- The Japan Society of Mechanical Engineers
- Society of Automotive Engineers of Japan

Awards:
- Outstanding Technical Paper Award of JSAE, 2004 and 2010

Jun'ichi Mizuta

Research Field:
- Diesel Engine Combustion

Academic Society:
- Society of Automotive Engineers of Japan

Awards:
- Outstanding Technical Paper Award of JSAE, 1997 and 2010

Kiyomi Nakakita

Research Fields:
- Diesel Engine
- Gasoline Engine
- Hybrid Electric Vehicle

Academic Degree: Dr. Eng.

Academic Societies:
- Society of Automotive Engineers of Japan
- The Japan Society of Mechanical Engineers
- Combustion Society of Japan
- Institution for Liquid Atomization and Spray Systems - Japan

Awards:
- Outstanding Technical Paper Award of JSAE, 1992, 2000 and 2005
- Engine Systems Memorial Award, the Engine Systems Div., JSME, 1996
- SAE 2003 Harry LeVan Horning Memorial Award, 2004

Shigeki Nakayama*

Research Field:
- Exhaust Aftertreatment

Academic Society:
- Society of Automotive Engineers of Japan

Awards:
- Outstanding Presentation Award of JSAE, 2007
- Outstanding Technical Paper Award of JSAE, 2010

*Toyota Motor Corporation

